Coherence Distillation Unveils Einstein-Podolsky-Rosen Steering

Kuan-Yi Lee,[1,2] Jhen-Dong Lin,[1,2,*] Karel Lemr,[3] Antonín Černoch,[4] Adam Miranowicz,[5,6] Franco Nori,[5,7,8] Huan-Yu Ku,[9,†] and Yueh-Nan Chen[1,2,5,‡]

[1] *Center for Quantum Frontiers of Research and Technology (QFort), National Cheng Kung University, Tainan 701, Taiwan*
[2] *Department of Physics, National Cheng Kung University, Tainan 701, Taiwan*
[3] *Palacký University in Olomouc, Faculty of Science, Joint Laboratory of Optics of Palacký University and Institute of Physics AS CR, 17. listopadu 12, 771 46 Olomouc, Czech Republic*
[4] *Institute of Physics of the Academy of Sciences of the Czech Republic, Joint Laboratory of Optics of Palacký University and Institute of Physics AS CR, 17. listopadu 50a, 772 07 Olomouc, Czech Republic*
[5] *Theoretical Quantum Physics Laboratory, Cluster for Pioneering Research, RIKEN Wakoshi, Saitama 351-0198, Japan*
[6] *Institute of Spintronics and Quantum Information, Faculty of Physics, Adam Mickiewicz University, 61-614 Poznań, Poland*
[7] *Center for Quantum Computing, RIKEN Wakoshi, Saitama 351-0198, Japan*
[8] *Department of Physics, The University of Michigan, Ann Arbor, 48109-1040 Michigan, USA*
[9] *Department of Physics, National Taiwan Normal University, Taipei 11677, Taiwan*

(Dated: December 5, 2023)

Quantum coherence is a fundamental property in quantum information science. Recent developments have provided valuable insights into its distillability and its relationship with nonlocal quantum correlations, such as quantum discord and entanglement. In this work, we focus on quantum steering and the local distillable coherence for a steered subsystem. We propose a steering inequality based on collaborative coherence distillation. Notably, we prove that the proposed steering witness can detect one-way steerable and all pure entangled states. Through linear optical experiments, we corroborate our theoretical efficacy in detecting pure entangled states. Furthermore, we demonstrate that the violation of the steering inequality can be employed as a quantifier of measurement incompatibility. Our work provides a clear quantitative and operational connection between coherence and entanglement, two landmark manifestations of quantum theory and both key enablers for quantum technologies.

arXiv:2312.01055v1 [quant-ph] 2 Dec 2023

Introduction.—Quantum coherence plays a pivotal role in quantum physics [1], which has spurred various applications in quantum information science, including cryptography [2], phase discrimination [3], and metrology [4]. Recently, the study of manipulating and quantifying quantum coherence has been developed under the framework of resource theory [5–11]. Several operational connections between local coherence and nonlocal quantum correlations, e.g., quantum discord and quantum entanglement, have been established [12–15]. In particular, it has been shown that nontrivial quantum discord can be harnessed to enhance the local distillable coherence through a collaborated coherence distillation task [8, 16, 17].

Aside from quantum discord and entanglement, quantum steering has also been identified as an intriguing quantum correlation, which plays an intermediate quantum phenomenon between entanglement [18–22] and Bell nonlocality [23–27]. Quantum steerability offers fundamental advantages for one-sided device-independent quantum information tasks, including subchannel discrimination [28], quantum key distribution [29], and quantum metrology [30, 31]. Recently, a notion termed "non-local advantage of quantum coherence" has been proposed, demonstrating that quantum steerability can enhance local coherence [32, 33]. However, the interplay between quantum steering and quantum coherence still remains an area that necessitates further exploration.

In this work, we propose a collaborated coherence distillation task assisted by quantum steering. We construct a steering inequality based on the distillable coherence and Shannon entropy of the steered subsystem. More specifically, we show that if the shared correlation is unsteerable, the local distillable coherence is upper bounded by the Shannon entropy. Therefore, if the distillable coherence exceeds the Shannon entropy, one can conclude that the correlation is steerable. In addition, we investigate the intricacies of the steering inequality violation (SIV). We show that the SIV exhibits several characteristics, such as (1) asymmetry, (2) the ability to detect all purely entangled states, and (3) a convex-decreasing function under a genuinely incoherent operation. By leveraging point (3), the proposed SIV can be used to quantify measurement incompatibility [34–36]. We also conduct linear optical experiments, demonstrating that the SIV can witness bipartite pure entangled states.

Distillable coherence.—In this section, we provide a concise overview of coherence distillation [17]. Given a priori reference basis $\{|i\rangle\}_i$, a quantum state ρ is considered incoherent if it is diagonal with respect to the reference basis, i.e., $\rho = \sum_i p_i |i\rangle\langle i|$, where p_i forms a probability distribution. Thus, states that are not in this form are categorized as coherent states [8]. We denote the set of incoherent states as $\mathcal{I}$. Furthermore, a quantum operation Λ is identified as a quantum-incoherent operation (QIO) if it maps an arbitrary incoherent state to another incoherent state. For the ease of expression, we sometimes extend the term QIO to refer to the set of

quantum incoherent operations.

A coherence distillation process involves the utilization of QIOs to convert n copies of general quantum states into the single-qubit maximally coherent state $|\Phi_2\rangle = \sum_{i=0}^{1} |i\rangle/\sqrt{2}$ with a rate R [17]. In the asymptotic limit, i.e., $n \to \infty$, the maximal rate is called the distillable coherence: $C_{\rm d}(\rho) = \sup\left\{R : \lim_{n\to\infty} \inf_{\Lambda\in{\rm QIO}} ||\Lambda(\rho^{\otimes n}) - \Phi_2^{\otimes Rn}|| = 0\right\}$, where $||\bullet||$ denotes the trace norm. As reported in Ref. [17], the distillable coherence has a closed form:

$$C_{\rm d}(\rho) = H_\Delta(\rho) - S(\rho), \tag{1}$$

where $S(\rho) = -{\rm Tr}\rho\log_2\rho$ is the von-Neumann entropy. Here, we adopt $H_\Delta(\rho) = S[\Delta(\rho)]$ as a shorthand notation, characterizing the Shannon entropy of the state under the reference basis, where $\Delta(\cdot) = \sum_i |i\rangle\langle i|\langle i|\cdot|i\rangle$ represents the complete decoherence operation, e.g. $\Delta(\rho) = \sum_i p_i |i\rangle\langle i|$. Note that a state ρ is distillable (i.e. $C_{\rm d} > 0$) if and only if $\rho \notin \mathcal{I}$.

It is worthwhile to interpret Eq. (1) from the perspective of "quantum uncertainty" described in Ref. [37]. Specifically, it is known that the von-Neumann entropy $S(\rho)$ characterizes the "classical part of uncertainty" as it aligns with the classical notion, where the uncertainty originates from the lack of information of a system. In addition, the Shannon entropy $H_\Delta(\rho)$ captures the "total uncertainty" or the observed uncertainty characterized by the probability distribution $\{p_i\}_i$. Therefore, according to Eq. (1), $C_d(\rho)$ quantifies the amount of observed uncertainty that cannot be explained by classical ignorance of the system. Along with this reasoning, the distillable coherence can be interpreted as quantum uncertainty. Through a rearrangement of Eq. (1), i.e., $C_d(\rho) + S(\rho) = H_\Delta(\rho)$, one can obtain an *uncertainty complementary relation*, where the total uncertainty is constituted by the quantum and classical uncertainties [37–40]. This implies the quantum uncertainty cannot exceed the total uncertainty, i.e.,

$$C_{\rm d}(\rho) \le H_\Delta(\rho). \tag{2}$$

The inequality is saturated when ρ is a pure state, given that there is no classical uncertainty. In the following, we show that this complementarity also holds when a bipartite system is unsteerable, while steerable states can violate this relation.

Steering-assisted coherence distillation.—We now characterize the steering-assisted coherence distillation task, as illustrated in Fig. 1. Suppose that Alice and Bob share a bipartite state ρ^{AB}. Alice performs a set of positive operator-valued measures (POVM), denoted as $\mathcal{M} = \{M_{a|x}\}_{a,x}$ satisfying $M_{a|x} \ge 0\ \forall\ a,x$ and $\sum_a M_{a|x} = \mathbb{1}\ \forall\ x$. Here, x denotes the measurement settings and a represents the corresponding outcomes. The measurement results can be succinctly represented by a conditional probability distribution $p(a|x)$. After the measurements, Alice communicates both the outcome a and the setting x to Bob, where we denote Bob's conditional state as $\rho_{a|x}$.

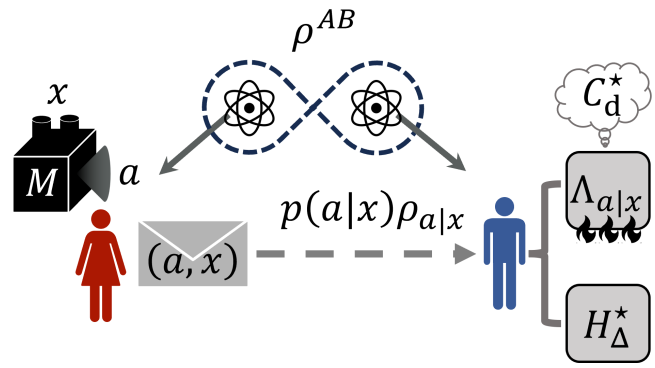

FIG. 1. Schematic illustration of the steering-assisted coherence distillation scenario. A bipartite system ρ^{AB} is shared by Alice and Bob. Alice measures her subsystem with measurement setting x and obtains outcome a with probability $p(a|x)$. After that, she sends the information (a,x) to Bob through classical communication. Depending on the measurement setting, Bob decides whether to perform coherence distillation or to compute the Shannon entropy.

The result can be characterized by a state assemblage. Quantum mechanically, it can be expressed as $\mathcal{A}$, which is defined by $\mathcal{A} = \{\sigma_{a|x}\}_{a,x}$ with $\sigma_{a|x} = p(a|x)\rho_{a|x}\ \forall\ a,x$. It is known that one can employ the local-hidden-state (LHS) model to determine whether a given assemblage is steerable or not. Specifically, an assemblage $\mathcal{A}^{\rm LHS}$ admits an LHS model when its elements can be described by [41]:

$$\sigma_{a|x}^{\rm LHS} = \sum_\lambda p(\lambda)p(a|x,\lambda)\rho_\lambda \quad \forall a,x, \tag{3}$$

where $\{\rho_\lambda\}_\lambda$ and $\{p(a|x,\lambda)\}_{a,x}$ are, respectively, hidden states and probabilities that constitute a stochastic process mapping the hidden variable λ into the observable outcomes $a|x$. For convenience, we also consider the state assemblage for a fixed setting x, denoted as $\mathcal{A}_x = \{\sigma_{a|x}\}_a$.

Based on Alice's measurement setting, Bob either distills the quantum coherence or computes the Shannon entropy under the reference basis. With the help of Alice's classical communication, Bob can adjust the local incoherent operation $\Lambda_{a|x}$ to optimize his distillable coherence. Here, we define the conditional distillable coherence and Shannon entropy for a given setting as x:

$$\begin{aligned} C_{\rm d}^{B|A}(\mathcal{A}_x) &= \sum_a p(a|x)C_{\rm d}(\rho_{a|x}) \\ H_\Delta^{B|A}(\mathcal{A}_x) &= \sum_a p(a|x)H_\Delta\left(\rho_{a|x}\right). \end{aligned} \tag{4}$$

By utilizing the convexity of $C_{\rm d}$, we show that the conditional distillable coherence can be upper-bounded for all

LHS models, namely, $C_{\rm d}^{B|A}(\mathcal{A}_x^{\rm LHS}) \leq \sum_\lambda p(\lambda) H_\Delta(\rho_\lambda)$. Likewise, the conditional Shannon entropy possesses a lower bound by its concavity, namely $H_\Delta^{B|A}(\mathcal{A}_x^{\rm LHS}) \geq \sum_\lambda p(\lambda) H_\Delta(\rho_\lambda)$. Therefore, we obtain the steering inequality:

$$C_{\rm d}^{B|A}(\mathcal{A}_x^{\rm LHS}) \leq H_\Delta^{B|A}(\mathcal{A}_{x'}^{\rm LHS}) \quad \forall\, x, x'. \tag{5}$$

In this sense, violation of this inequality implies the given state is steerable. Equation (5) can be regarded as a generalization of the complementarity relation of uncertainty described in Eq. (2). Consequently, the proposed witness suggests that *quantum steerability can be captured as the violation of the complementarity of uncertainty.*

Properties of the steering inequality violation (SIV).— Here we consider the SIV, which is defined as

$$\mathcal{V}_{\rm S}(\mathcal{A}) := \max\left\{\max_x C_{\rm d}^{B|A}(\mathcal{A}_x) - \min_x H_\Delta^{B|A}(\mathcal{A}_x), 0\right\}, \tag{6}$$

where $\max\{x_1, x_2\} = x_1$, if $x_1 > x_2$; $\max\{x_1, x_2\} = x_2$ otherwise. By this definition, the SIV vanishes if the given state assemblage admits a LHS model. Furthermore, we show that the SIV satisfies the following properties, and the proofs can be found in Supplemental Material [42].

Property 1.—The SIV is asymmetric. In the sense that the values of SIV are different for Alice to Bob and vice versa.

A steering test should be naturally asymmetrical, and this distinction becomes evident as discussed in previous works [43–45] that permits steering occurrs in a unidirectional manner, specifically, from Alice to Bob.

With this property in hand, we can directly show the following.

Corollary 2.—The SIV can detect one-way steering.

In the steering scenario, Alice and Bob each have distinct roles. Therefore, the presence of steerability in one direction (from Alice to Bob) does not guarantee its existence in the opposite direction (from Bob to Alice) [43, 44]. Several examples are provided in the Supplemental Material [42].

Property 3.—The SIV can detect all pure entangled states.

It is known that all pure entangled states are steerable [41]. This aspect can also be revealed by the SIV. More specifically, we show that for all pure bipartite entangled state $|\psi\rangle^{AB} = \sum_i \sqrt{p_i}\,|i\rangle \otimes |i\rangle$, there exists a set of Alice's measurement and a reference basis $\{|i\rangle\}_i$ s.t. $\mathcal{V}_{\rm S} > 0$ [42].

This property showcases that SIV is also a witness of entanglement when evaluated on pure entangled states and is distinct from other coherence-based steering inequality [32]. We also show the experimental demonstration of the steering violation for the pure entangled state later.

One can ask whether the SIV can serve as a steering monotone [46]. The answer is negative, because SIV does not generally monotonically decrease under one-way local operations and classical communications [42] (see Supplemental Material for an example). However, the SIV could be non-increasing if we restrict the local operations to QIOs [8, 16, 17] as suggested by the numerical results included in Supplemental Material [42]. In the following property, we prove that SIV is a non-increasing function under genuine incoherent operations (GIOs), which form a subset of QIO [47].

Property 4.—The SIV is a convex-decreasing function under genuine incoherent operations.

According to Ref. [47], there exists a Kraus representation of a GIO such that all Kraus operators of the GIO are diagonalized with respect to the reference basis. Using this property, one can show that distillable coherence (Shannon entropy) monotonically decreases (increases) under GIO, implying that $\mathcal{V}_{\rm S}$ also monotonically decreases under GIO [42]. With this property, one can further show that SIV is non-increasing under one-way local GIO and classical communications.

Quantify measurement incompatibility.—In this section, we show that the SIV can be used to quantify measurement incompatibility [34, 35, 48–50]. Incompatible measurements, which represent that multiple physical quantities cannot be measured simultaneously, is a fundamental characteristic arising from various quantum phenomena [51, 52]. Given a set of POVMs $\mathcal{M} = \{M_{a|x}\}_{a,x}$, it is compatible (or jointly measurable) if it can be expressed by

$$M_{a|x} = \sum_\lambda p(a|x,\lambda) G_\lambda, \tag{7}$$

where $\{G_\lambda\}_\lambda$ is a parent POVM and $p(a|x,\lambda)$ is conditional probability. One can observe that the joint measurable model and the LHS model in Eq. (3) share a mathematical similarity. Given a state assemblage, it can be transmitted to a set of POVMs via the concept of the steering-equivalent observables (SEO) $\mathcal{B} = \{B_{a|x}\}_{a,x}$ i.e., $B_{a|x} = (\rho_B)^{-1/2}\sigma_{a|x}(\rho_B)^{-1/2}$ with $\rho_B = \sum_a \sigma_{a|x}$ [53]. We note that once ρ_B is not full rank, the same expression can be obtained by considering an additional isometry (see also Ref. [53]). One can see that the SEO is incompatible if and only if the state assemblage is steerable [53].

Inspired by the very recently proposed steering-induced incompatible measure [49], we are able to quantify measurement incompatibility by the steering-assisted coherence distillation, namely

$$\mathcal{V}_{\rm I}(\mathcal{B}) = \sup_{\rho_B} \mathcal{V}_{\rm S}[\sqrt{\rho_B}\ \mathcal{B}\sqrt{\rho_B}], \tag{8}$$

where sup is taking over all full-rank states ρ_B, and $\mathcal{V}_{\rm S}$ is SIV defined in Eq. (6). We then can show the following:

Property 5.—The optimal steering-assisted coherence distillation $\mathcal{V}_{\rm I}(\mathcal{B})$ is a valid incompatibility monotone [34] in the sense that it satisfies: (a) $\mathcal{V}_{\rm I}(\mathcal{B}) = 0$ if $\mathcal{B} \in$ jointly measurable; (b) $\mathcal{V}_{\rm I}(\mathcal{B})$ satisfies convexity; (c) $\mathcal{V}_{\rm I}(\mathcal{B})$ is non-increasing under post-processing, namely

$$\begin{aligned}\{B_{a'|x'}\}_{a',x'} &= \mathcal{W}(\{B_{a|x}\}_{a,x}) \\ &= \sum_{a,x} p(x|x')p(a'|a,x,x')\{B_{a|x}\}_{a,x},\end{aligned} \tag{9}$$

where $p(x|x')$ and $p(a'|a,x,x')$ are the conditional probabilities and $\mathcal{W}$ is a post-processing scenario defined as a deterministic wiring map [46]. The proofs can be found in Supplemental Material [42].

This result further strengthens the application of the steering-assisted coherence distillation. In one direction, it quantitatively connects measurement incompatibility with quantum coherence and gives an additional concrete example for steering-induced incompatible measure [50] In the other direction, we clearly provide a different operational interpretation of measurement incompatibility. Specifically, if we consider ρ^{AB} is a pure entangled state, the SEO $\mathcal{B}$ of $\mathcal{A}$ generated by $\mathcal{M}$ is exactly equivalent to $\mathcal{M}$. In this sense, the measurement incompatibility of $\mathcal{M}$ can be accessed in a steering-assisted coherence distillation by properly choosing the pure state ρ^{AB} such that $\mathcal{V}_{\rm I}(\mathcal{M}) = \sup_{\rho_B} \mathcal{V}_{\rm S}[\sqrt{\rho_B}\mathcal{M}\sqrt{\rho_B}]$.

Experimental demonstration—To support the derived theoretical framework, we have performed experimental testing on the platform of linear optics encoding two-qubit states into polarizations of photon pairs. The experimental setup, as depicted in Fig. 2(a), consists of a laser emitting pulses at 355 nm that impinge into a crystal cascade made of two β-BaB_2O_4 crystals (2×BBO). These crystals are 1 mm thick and are mutually positioned so that their optical axes lie in mutually perpendicular planes [54]. In these crystals, the laser beam is subjected to the nonlinear process of type-I spontaneous parametric down-conversion (SPDC). In the first crystal, horizontally polarized laser photons are converted into pairs of vertically polarized photons at 710 nm. The second crystal facilitates creation of horizontally-polarized photon pairs from the vertically polarized laser beam. Photon pairs generated in both crystals are subsequently collected into single-mode optical fibers. Coherence of the laser beam and indistinguishability in the photons collection assure the effective generation of the photon pairs in a superposition state of both contributing processes, $|\Phi\rangle = \frac{1}{\sqrt{2}}\left(\sqrt{q}|HH\rangle + {\rm e}^{{\rm i}\phi}\sqrt{1-q}|VV\rangle\right)$, where H and V stand for the horizontal and vertical polarization states, respectively. Parameters q and ϕ are controlled by tuning the laser-beam polarization using half- and quarter-wave plates.

The aforementioned single-mode fibers guide the photon pairs to the state detection and the analysis part of the setup. A series of half- and quarter-wave plates followed by a polarizer implement local projections onto any pure polarization state. Such polarization projection is implemented independently on both photons of a pair. We project the photon pairs onto all the combinations of the eigenstates of the Pauli matrices and register the number of simultaneous two-photon detections for all these combinations [55]. A method of maximum likelihood is then used to estimate the most probable density matrix fitting the registered counts [56]. This density matrix is then used to calculate the corresponding SIV.

To evaluate the experimental uncertainty of the calculated SIV, we make use of the fact that registered photon detections follow the Poisson statistics (shot-noise). A Monte-Carlo method is implemented, where all registered counts are randomized assuming the Poisson statistics with the mean value being the actual experimentally observed value. Subsequently the maximum-likelihood method is deployed to estimate the density matrix, which is then used to calculate the SIV. By repeating this procedure 1000 times, we obtain the statistics of the SIV under the detection shot-noise and establish the confidence intervals, $\pm\sigma$.

Any experimental implementation is, at least to some degree, imperfect. Partial distinguishability in the generating crystal and imperfections of polarization optics lead to non-unit purity of the generated states. These imperfections can be reasonably well modeled by white noise. To estimate the amount of such noise, we maximize the expression $F(\rho_{p_0}, \rho_{\rm exp}) = \max_p({\rm Tr}\sqrt{\sqrt{\rho_p}\rho_{\rm exp}\sqrt{\rho_p}})^2$, where F denotes the Bures fidelity, $\rho_{\rm exp}$ is the experimentally observed density matrix and $\rho_p = (1-p)\rho_{\rm th} + p\mathbb{1}/4$ is the theoretical density matrix $\rho_{\rm th}$ with added white noise. We have found that for the series of the noisy quasi-pure states ρ_p and presented in Fig. 2(b), the optimal value of p is $p_0 = 0.026$ on average.

In Fig. 2(b), we compare the theoretical predictions with the experimental results. The noise-free theoretical predictions, i.e., ${\rm SIV}(q) = q\log_2 q + (1-q)\log_2(1-q)$, are represented as the black solid line. Note that ${\rm SIV}(q) > 0$ if $q > 0$. The predictions with a noise factor $p_0 = 0.026$ are represented as the black-dash lines. The experimental results are shown in blue cubes with error bars obtained via the above mentioned Monte-Carlo method.

Discussions and Conclusions.—We propose a quantum steering inequality based on coherence distillation, where the inequality is formulated as an uncertainty complementary relation. We theoretically show that our approach is capable of detecting all bipartite pure entangled states, and the SIV is asymmetric, enabling the detection of one-way steerability. We also demonstrate the SIV is convex in assemblage and non-increasing under post-processing. With these properties in hand, we extend the application of the SIV such that it can be used to quantify steering-induced measurement incompatibility. Finally, we experimentally demonstrated the ability of the SIV to detect bipartite pure entangled states.

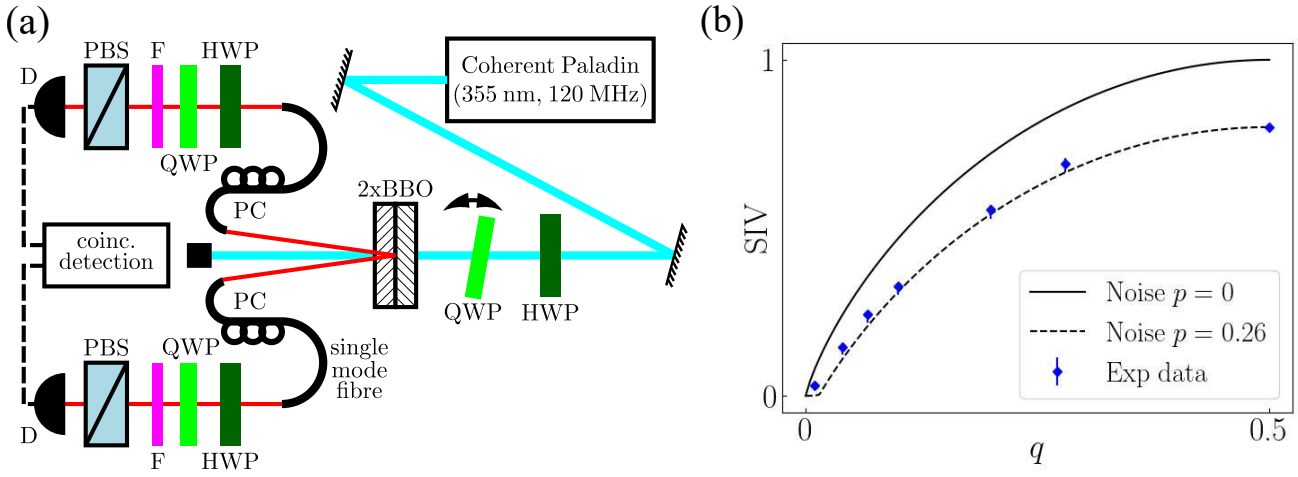

FIG. 2. (a) Schematic representation of the experimental setup. Individual components are labelled as follows: BBO – β-BaB_2O_4 crystal, HWP – half-wave plate, QWP – quarter-wave plate, F – interference bandpass filter (5 nm spectral width), PBS – polarizer, PC – fiber polarization controller, D – single-photon avalanche photodiode. (b) The theoretical predictions are juxtaposed with the experimental results. The black solid line illustrates the noise-free theoretical outcomes given by $\mathrm{SIV}(q) = q\log_2 q + (1-q)\log_2(1-q)$; meanwhile, the black-dash lines represent the theoretical predictions incorporating a noise factor $p_0 = 0.026$; the blue cubes indicate experimental results, with error bars obtained via the Monte-Catlo method as described in the text.

Moreover, we demonstrate that the SIV is monotonic under the restricted local operations. Nevertheless, the validation of SIV as a steering monotone remains an open question. If the SIV is a valid convex steering monotone, it would stand as an efficient measure, given that the SIV avoids using optimization methods like semi-definite programming that demands significant computational resources.

It has been shown that the framework of asymptotic distillation of coherence can be extended to one-shot [57, 58] and asymptotic reversibility settings [59]. It raises an intriguing question: can these distillation scenarios also detect and possibly quantify quantum steering?

Acknowledgements.—We are grateful to Eric Chitambar for fruitful discussion. A.M. is supported by the Polish National Science Centre (NCN) under the Maestro Grant No. DEC-2019/34/A/ST2/00081. F.N. is supported in part by: Nippon Telegraph and Telephone Corporation (NTT) Research, the Japan Science and Technology Agency (JST) [via the Quantum Leap Flagship Program (Q-LEAP), and the Moonshot R&D Grant Number JPMJMS2061], the Japan Society for the Promotion of Science (JSPS) [via the Grants-in-Aid for Scientific Research (KAKENHI) Grant No. JP20H00134], the Army Research Office (ARO) (Grant No. W911NF-18-1-0358), the Asian Office of Aerospace Research and Development (AOARD) (via Grant No. FA2386-20-1-4069), and the Foundational Questions Institute Fund (FQXi) via Grant No. FQXi-IAF19-06. H.-Y. K. is supported by the Ministry of Science and Technology, Taiwan, (Grants No. MOST 111-2917-I-564-005, 112-2112-M-003 -020 -MY3, and), and Higher Education Sprout Project of National Taiwan Normal University (NTNU) and the Ministry of Education (MOE) in Taiwan. This work is supported by the National Center for Theoretical Sciences and National Science and Technology Council, Taiwan, Grants No. NSTC 112-2123-M-006-001.

* jhendonglin@gmail.com
† huan.yu@ntnu.edu.tw
‡ yuehnan@mail.ncku.edu.tw

[1] A. Streltsov, G. Adesso, and M. B. Plenio, Colloquium: Quantum coherence as a resource, Rev. Mod. Phys. **89**, 041003 (2017).
[2] P. J. Coles, E. M. Metodiev, and N. Lütkenhaus, Numerical approach for unstructured quantum key distribution, Nat. Commun. **7**, 11712 (2016).
[3] C. Napoli, T. R. Bromley, M. Cianciaruso, M. Piani, N. Johnston, and G. Adesso, Robustness of coherence: An operational and observable measure of quantum coherence, Phys. Rev. Lett. **116**, 150502 (2016).
[4] C. Zhang, T. R. Bromley, Y.-F. Huang, H. Cao, W.-M. Lv, B.-H. Liu, C.-F. Li, G.-C. Guo, M. Cianciaruso, and G. Adesso, Demonstrating quantum coherence and metrology that is resilient to transversal noise, Phys. Rev. Lett. **123**, 180504 (2019).
[5] S. Luo, Wigner-yanase skew information and uncertainty relations, Phys. Rev. Lett. **91**, 180403 (2003).
[6] S. Luo and Q. Zhang, On skew information, IEEE Transactions on Information Theory **50**, 1778 (2004).
[7] J. Aberg, Quantifying superposition, arXiv:quant-ph/0612146 (2006).
[8] T. Baumgratz, M. Cramer, and M. B. Plenio, Quantifying coherence, Phys. Rev. Lett. **113**, 140401 (2014).
[9] F. Levi and F. Mintert, A quantitative theory of coherent

delocalization, New J. Phys. **16**, 033007 (2014).
[10] T. R. Bromley, M. Cianciaruso, and G. Adesso, Frozen quantum coherence, Phys. Rev. Lett. **114**, 210401 (2015).
[11] M. N. Bera, Quantifying superpositions of quantum evolutions, Phys. Rev. A **100**, 042307 (2019).
[12] A. Streltsov, U. Singh, H. S. Dhar, M. N. Bera, and G. Adesso, Measuring quantum coherence with entanglement, Phys. Rev. Lett. **115**, 020403 (2015).
[13] J. Ma, B. Yadin, D. Girolami, V. Vedral, and M. Gu, Converting coherence to quantum correlations, Phys. Rev. Lett. **116**, 160407 (2016).
[14] X. Hu, A. Milne, B. Zhang, and H. Fan, Quantum coherence of steered states, Sci. Rep. **6**, 19365 (2016).
[15] X. Hu and H. Fan, Extracting quantum coherence via steering, Sci. Rep. **6**, 34380 (2016).
[16] E. Chitambar, A. Streltsov, S. Rana, M. N. Bera, G. Adesso, and M. Lewenstein, Assisted distillation of quantum coherence, Phys. Rev. Lett. **116**, 070402 (2016).
[17] A. Winter and D. Yang, Operational resource theory of coherence, Phys. Rev. Lett. **116**, 120404 (2016).
[18] R. Horodecki, P. Horodecki, M. Horodecki, and K. Horodecki, Quantum entanglement, Rev. Mod. Phys. **81**, 865 (2009).
[19] M. F. Pusey, Negativity and steering: A stronger peres conjecture, Phys. Rev. A **88**, 032313 (2013).
[20] D. Cavalcanti and P. Skrzypczyk, Quantitative relations between measurement incompatibility, quantum steering, and nonlocality, Phys. Rev. A **93**, 052112 (2016).
[21] H.-Y. Ku, J. Kadlec, A. Černoch, M. T. Quintino, W. Zhou, K. Lemr, N. Lambert, A. Miranowicz, S.-L. Chen, F. Nori, and Y.-N. Chen, Quantifying quantumness of channels without entanglement, PRX Quantum **3**, 020338 (2022).
[22] M. Fadel and M. Gessner, Entanglement of local hidden states, Quantum **6**, 651 (2022).
[23] N. Brunner, D. Cavalcanti, S. Pironio, V. Scarani, and S. Wehner, Bell nonlocality, Rev. Mod. Phys. **86**, 419 (2014).
[24] S.-L. Chen, C. Budroni, Y.-C. Liang, and Y.-N. Chen, Natural framework for device-independent quantification of quantum steerability, measurement incompatibility, and self-testing, Phys. Rev. Lett. **116**, 240401 (2016).
[25] M. T. Quintino, C. Budroni, E. Woodhead, A. Cabello, and D. Cavalcanti, Device-independent tests of structures of measurement incompatibility, Phys. Rev. Lett. **123**, 180401 (2019).
[26] Y.-Y. Zhao, H.-Y. Ku, S.-L. Chen, H.-B. Chen, F. Nori, G.-Y. Xiang, C.-F. Li, G.-C. Guo, and Y.-N. Chen, Experimental demonstration of measurement-device-independent measure of quantum steering, npj Quantum Inf. **6**, 77 (2020).
[27] S.-L. Chen, H.-Y. Ku, W. Zhou, J. Tura, and Y.-N. Chen, Robust self-testing of steerable quantum assemblages and its applications on device-independent quantum certification, Quantum **5**, 552 (2021).
[28] M. Piani and J. Watrous, Necessary and sufficient quantum information characterization of Einstein-Podolsky-Rosen steering, Phys. Rev. Lett. **114**, 060404 (2015).
[29] C. Branciard, E. G. Cavalcanti, S. P. Walborn, V. Scarani, and H. M. Wiseman, One-sided device-independent quantum key distribution: Security, feasibility, and the connection with steering, Phys. Rev. A **85**, 010301 (2012).
[30] B. Yadin, M. Fadel, and M. Gessner, Metrological complementarity reveals the Einstein-Pdolsky-Rosen paradox, Nat. Commun. **12**, 2410 (2021).
[31] K.-Y. Lee, J.-D. Lin, A. Miranowicz, F. Nori, H.-Y. Ku, and Y.-N. Chen, Steering-enhanced quantum metrology using superpositions of noisy phase shifts, Phys. Rev. Res. **5**, 013103 (2023).
[32] D. Mondal, T. Pramanik, and A. K. Pati, Nonlocal advantage of quantum coherence, Phys. Rev. A **95**, 010301 (2017).
[33] M.-L. Hu and H. Fan, Nonlocal advantage of quantum coherence in high-dimensional states, Phys. Rev. A **98**, 022312 (2018).
[34] P. Skrzypczyk, I. Šupić, and D. Cavalcanti, All sets of incompatible measurements give an advantage in quantum state discrimination, Phys. Rev. Lett. **122**, 130403 (2019).
[35] F. Buscemi, E. Chitambar, and W. Zhou, Complete resource theory of quantum incompatibility as quantum programmability, Phys. Rev. Lett. **124**, 120401 (2020).
[36] O. Gühne, E. Haapasalo, T. Kraft, J.-P. Pellonpää, and R. Uola, Colloquium: Incompatible measurements in quantum information science, Rev. Mod. Phys. **95**, 011003 (2023).
[37] Y. Sun and S. Luo, Coherence as uncertainty, Phys. Rev. A **103**, 042423 (2021).
[38] D. Girolami, T. Tufarelli, and G. Adesso, Characterizing nonclassical correlations via local quantum uncertainty, Phys. Rev. Lett. **110**, 240402 (2013).
[39] D. Girolami, Observable measure of quantum coherence in finite dimensional systems, Phys. Rev. Lett. **113**, 170401 (2014).
[40] R. M. Angelo and A. D. Ribeiro, Wave–particle duality: An information-based approach, Found. Phys. **45**, 1407 (2015).
[41] H. M. Wiseman, S. J. Jones, and A. C. Doherty, Steering, entanglement, nonlocality, and the Einstein-Podolsky-Rosen paradox, Phys. Rev. Lett. **98**, 140402 (2007).
[42] See supplemental material for further proofs and examples, .
[43] J. Bowles, T. Vértesi, M. T. Quintino, and N. Brunner, One-way einstein-podolsky-rosen steering, Phys. Rev. Lett. **112**, 200402 (2014).
[44] J. Bowles, F. Hirsch, M. T. Quintino, and N. Brunner, Sufficient criterion for guaranteeing that a two-qubit state is unsteerable, Phys. Rev. A **93**, 022121 (2016).
[45] R. Uola, A. C. S. Costa, H. C. Nguyen, and O. Gühne, Quantum steering, Rev. Mod. Phys. **92**, 015001 (2020).
[46] R. Gallego and L. Aolita, Resource theory of steering, Phys. Rev. X **5**, 041008 (2015).
[47] B. Yadin, J. Ma, D. Girolami, M. Gu, and V. Vedral, Quantum processes which do not use coherence, Phys. Rev. X **6**, 041028 (2016).
[48] H.-Y. Ku, C.-Y. Hsieh, S.-L. Chen, Y.-N. Chen, and C. Budroni, Complete classification of steerability under local filters and its relation with measurement incompatibility, Nat. Commun. **13**, 4973 (2022).
[49] C.-Y. Hsieh, H.-Y. Ku, and C. Budroni, Characterisation and fundamental limitations of irreversible stochastic steering distillation, arXiv.2309.06191 (2023).
[50] H.-Y. Ku, C.-Y. Hsieh, and C. Budroni, Measurement incompatibility cannot be stochastically distilled, arXiv.2308.02252 (2023).

[51] P. Busch, P. Lahti, and R. F. Werner, Colloquium: Quantum root-mean-square error and measurement uncertainty relations, Rev. Mod. Phys. **86**, 1261 (2014).
[52] O. Gühne, E. Haapasalo, T. Kraft, J.-P. Pellonpää, and R. Uola, Colloquium: Incompatible measurements in quantum information science, Rev. Mod. Phys. **95**, 011003 (2023).
[53] R. Uola, C. Budroni, O. Gühne, and J.-P. Pellonpää, One-to-one mapping between steering and joint measurability problems, Phys. Rev. Lett. **115**, 230402 (2015).
[54] P. G. Kwiat, E. Waks, A. G. White, I. Appelbaum, and P. H. Eberhard, Ultrabright source of polarization-entangled photons, Phys. Rev. A **60**, R773 (1999).
[55] E. Halenková, A. Černoch, K. Lemr, J. Soubusta, and S. Drusová, Experimental implementation of the multifunctional compact two-photon state analyzer, Appl. Opt. **51**, 474 (2012).
[56] M. Ježek, J. Fiurášek, and Z. Hradil, Quantum inference of states and processes, Phys. Rev. A **68**, 012305 (2003).
[57] B. Regula, K. Fang, X. Wang, and G. Adesso, One-shot coherence distillation, Phys. Rev. Lett. **121**, 010401 (2018).
[58] Q. Zhao, Y. Liu, X. Yuan, E. Chitambar, and A. Winter, One-shot coherence distillation: Towards completing the picture, IEEE Transactions on Information Theory **65**, 6441 (2019).
[59] E. Chitambar, Dephasing-covariant operations enable asymptotic reversibility of quantum resources, Phys. Rev. A **97**, 050301 (2018).
[60] H.-Y. Ku, S.-L. Chen, C. Budroni, A. Miranowicz, Y.-N. Chen, and F. Nori, Einstein-Podolsky-Rosen steering: Its geometric quantification and witness, Phys. Rev. A **97**, 022338 (2018).

Proof of the steering inequality

For convenience, we define the optimal conditional distillable coherence and optimal conditional Shannon entropy as

$$C_{\mathrm{d}}^{\star}(\mathcal{A}) := \max_x C_{\mathrm{d}}^{B|A}(\mathcal{A}_x) \quad \text{and} \quad H_{\Delta}^{\star}(\mathcal{A}) := \min_x H_{\Delta}^{B|A}(\mathcal{A}_x). \tag{10}$$

Proof. —The inequality $C_{\mathrm{d}}^{\star}(\mathcal{A}) \leq H_{\Delta}^{\star}(\mathcal{A})$ holds if the assemblage $\mathcal{A}$ admits LHS model.

Considering the assemblage Bob received can be described by LHS model, the upper bound of coherence distillation can be readily obtained, as such derivation:

$$\begin{aligned}
C_{\mathrm{d}}^{\star}(\mathcal{A}) &= \max_x \sum_a p(a|x) C_{\mathrm{d}} \left[\sum_\lambda p(\lambda|a,x)\rho_\lambda \right] \\
&= \max_x \sum_a p(a|x) C_{\mathrm{d}} \left[\sum_\lambda \frac{p(a|x,\lambda)p(\lambda)}{p(a|x)} \rho_\lambda \right] \\
&\leq \max_x \sum_a p(a|x) \sum_\lambda \frac{p(a|x,\lambda)p(\lambda)}{p(a|x)} C_{\mathrm{d}}(\rho_\lambda) \\
&= \max_x \sum_\lambda p(\lambda) C_{\mathrm{d}}(\rho_\lambda) \\
&= \sum_\lambda p(\lambda) C_{\mathrm{d}}(\rho_\lambda) \\
&\leq \sum_\lambda p(\lambda) H_{\Delta}(\rho_\lambda).
\end{aligned} \tag{11}$$

By the fact that $H_{\Delta}(\rho)$ is concave in ρ, we readily obtain $\sum_\lambda p(\lambda) H_{\Delta}(\rho_\lambda) \leq H_{\Delta}^{\star}(\mathcal{A})$ by analogous derivation, concluding the proof of steering inequality that

$$C_{\mathrm{d}}^{\star}(\mathcal{A}) \leq H_{\Delta}^{\star}(\mathcal{A}) \quad \text{if } \mathcal{A} \in \text{LHS}. \tag{12}$$

□

Proof of property 1

Proof. —SIV is asymmetric.

To demonstrate the asymmetry, we consider a two-qubit states defined by

$$\chi(\vec{r},\vec{s},\vec{t}) = \frac{1}{4}\left(\mathbb{1}\otimes\mathbb{1} + \vec{r}\cdot\vec{\sigma}\otimes\mathbb{1} + \mathbb{1}\otimes\vec{s}\cdot\vec{\sigma} + \sum_{i,j=0}^{2} t_{ij}\hat{\sigma}_i\otimes\hat{\sigma}_j\right), \tag{13}$$

where $\{\vec{r},\vec{s},\vec{t}\}$ are the vectors with norm less than unit and $\vec{\sigma} = (\hat{\sigma}_0,\hat{\sigma}_1,\hat{\sigma}_2)$ is Pauli vector. If SIV is asymmetric, the value of SIV will depend on the local Block vector, i.e., $\vec{r}$ and $\vec{s}$. Here, we consider Alice performs measurements described as $M_{a|x} = [\mathbb{1}_2 + (-1)^a\hat{\sigma}_x]/2$ with $a\in\{0,1\}$ and $x\in\{0,1\}$, where $\hat{\sigma}_0$ and $\hat{\sigma}_1$ are Pauli-Z and Pauli-X matrices, respectively, then the assemblage Bob received becomes

$$\begin{aligned}
\sigma_{a|x} &= \mathrm{Tr}_A\left[M_{a|x}\otimes\mathbb{1}\chi(\vec{r},\vec{s},\vec{t})\right]\\
&= \frac{1}{4}\mathrm{Tr}_A\left[M_{a|x}\otimes\mathbb{1} + M_{a|x}\vec{r}\cdot\vec{\sigma}\otimes\mathbb{1} + M_{a|x}\otimes\vec{s}\cdot\vec{\sigma} + \sum_{i,j=0}^{2} M_{a|x}t_{ij}\hat{\sigma}_i\otimes\hat{\sigma}_j\right]\\
&= \frac{1}{4}\left\{\mathbb{1} + \frac{1}{2}\mathrm{Tr}\left[\vec{r}\cdot\vec{\sigma} + (-1)^a\hat{\sigma}_x\vec{r}\cdot\vec{\sigma}\right]\mathbb{1} + \vec{s}\cdot\vec{\sigma} + \frac{1}{2}\sum_{i,j=0}^{2} t_{ij}\mathrm{Tr}\left[\hat{\sigma}_i + (-1)^a\hat{\sigma}_x\hat{\sigma}_i\right]\hat{\sigma}_j\right\}\\
&= \frac{1}{4}\left[\mathbb{1} + (-1)^a r_x\mathbb{1} + \vec{s}\cdot\vec{\sigma} + \sum_j (-1)^a t_{xj}\sigma_j\right]\\
&= \frac{1}{2}\left[1 + (-1)^a r_x\right]\times\frac{1}{2}\left[\mathbb{1} + \sum_j \frac{s_j + (-1)^a t_{xj}}{1 + (-1)^a r_x}\sigma_j\right]
\end{aligned} \tag{14}$$

with probability $\mathrm{Tr}\sigma_{a|x} = [1 + (-1)^a r_x]/2$ and the latter term in Eq.(14) is the conditional state $\rho_{a|x}$. To obtain the SIV, we need to calculate the eigenvalue of the reduced state $\rho_{a|x}$ and its dephased counterpart $\Delta(\rho_{a|x}) = \sum_{i=0}^{1}\langle i|\rho_{a|x}|i\rangle|i\rangle\langle i|$, which are, respectively,

$$E_{a|x,\pm}(r,s,t) = \frac{1}{2}\left[1 \pm \frac{\sqrt{\sum_j\left[s_j + (-1)^a t_{xj}\right]^2}}{1 + (-1)^a r_x}\right] \quad \text{and} \quad E^{\mathrm{deph}}_{a|x,\pm}(r,s,t) = \frac{1}{2}\left[1 \pm \frac{s_0 + (-1)^a t_x\delta_{x,0}}{1 + (-1)^a r_x}\right]. \tag{15}$$

Here, we can observe that the SIV depends on the local Block vector $\vec{r}$ and $\vec{s}$, meaning that after we SWAP the two-qubit states $\chi(\vec{r},\vec{s},\vec{t})$ into $\chi(\vec{s},\vec{r},\vec{t})$, the SIV will alter. □

Example of corollary 2: The SIV can detect one-way steering

As a concrete example, we present the SIV of a set of states described by

$$\chi(s,q) = s|\psi_q\rangle\langle\psi_q| + (1-s)\mathrm{Tr}_B\left(|\psi_q\rangle\langle\psi_q|\right)\otimes\mathbb{1}/2, \tag{16}$$

where $|\psi_q\rangle = \sum_{i=0}^{1} t_i(q)|i\rangle\otimes|i\rangle$ and $t_0(q) = q,\ t_1(q) = 1-q$ in the parameter windows: $s\in[0.75,1]$ and $q\in[0.001,0.5]$. The SIV values are shown in Fig. 3. In light-red area (I), the steerability can be detected from both directions, i.e., $\mathcal{V}_{\mathrm{S}}(\mathcal{A}^{B\to A}) > 0$ and $\mathcal{V}_{\mathrm{S}}(\mathcal{A}^{A\to B}) > 0$. However, in the light-blue area (II), one finds $\mathcal{V}_{\mathrm{S}}(\mathcal{A}^{B\to A}) = 0$, while $\mathcal{V}_{\mathrm{S}}(\mathcal{A}^{B\to A}) > 0$, which indicates that the SIV is only witnessed from Bob to Alice. Finally, in the grey area (III), the steerability cannot be detected from any directions.

Proof of property 3

Proof. —For all pure bipartite entangled state, there exists a set of Alice's measurement and a reference basis such that SIV > 0.

Let us consider a set of projective measurements $\{\Pi_{a|x}\}_{a,x}$ for $a,x\in\{0,1\}$, with one of which (label as $x=0$) satisfies

$$\Pi_{a|x=0}|i\rangle = \delta_{ia}|i\rangle. \tag{17}$$

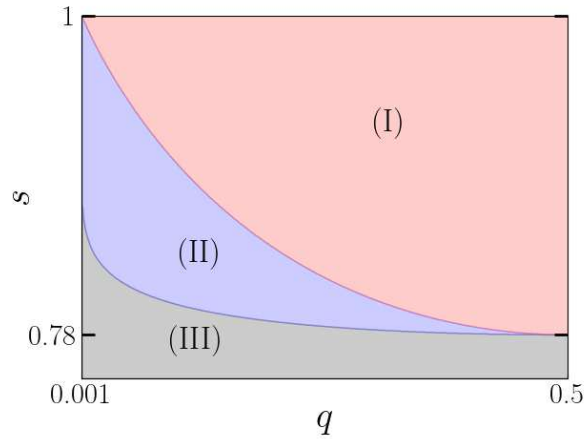

FIG. 3. Ability of the SIV to demonstrate one-way quantum steering. The light-red area (I) represents both $\mathcal{V}_{\rm S}(\mathcal{A}^{B\to A})>0$ and $\mathcal{V}_{\rm S}(\mathcal{A}^{A\to B})>0$, suggesting that quantum steering occurs in both directions. The light-blue area (II), conversely, represents $\mathcal{V}_{\rm S}(\mathcal{A}^{B\to A})>0$ but $\mathcal{V}_{\rm S}(\mathcal{A}^{A\to B})=0$, indicating that the respective steerable state only allows Bob to steer Alice. Finally, the grey area (III) represents the range that $\mathcal{V}_{\rm S}(\mathcal{A}^{B\to A})=0$ and $\mathcal{V}_{\rm S}(\mathcal{A}^{A\to B})=0$.

This specific measurement $\Pi_{a|x=0}$ on Alice system causes the conditional state $|\psi\rangle_{a|x=0} = {\rm Tr}_A\Pi_{a|x=0}\otimes \mathbb{1}\,|\psi\rangle^{AB}/{\rm Tr}\Pi_{a|x=0}\otimes\mathbb{1}\,|\psi\rangle^{AB}$ to a pure and incoherent state. Given that all the conditional states $|\psi\rangle_{a|x}$ remain pure states, we have

$$\begin{aligned} C^{\star}_{\rm d}(\mathcal{A}) &= \max_x \sum_a p(a|x) H_\Delta(|\psi\rangle_{a|x}) \\ \text{and } H^{\star}_{\Delta}(\mathcal{A}) &= \min_x \sum_a p(a|x) H_\Delta(|\psi\rangle_{a|x}) = 0, \end{aligned} \tag{18}$$

in which $H^{\star}_{\Delta}(\mathcal{A})=0$ is due to the fact that for all pure states $|\psi\rangle$, $H_\Delta(|\psi\rangle)=0$ if and only if $\Delta(|\psi\rangle)=|\psi\rangle$. By setting another projective measurement $\{\Pi_{a|x=1}\}_a$ not commute with $\{\Pi_{a|x=0}\}_a$, i.e., $[\sum_a a\Pi_{a|x=0}, \sum_{a'} a'\Pi_{a'|x=1}]\neq 0$, we can ensure $C^{\star}_{\rm d}(\mathcal{A})>0$ and, therefore, conclude that $\mathcal{V}_{\rm S}>0$. □

Proof of incompatibility monotone

$\mathcal{V}_{\rm I}(\mathcal{M})$ is a valid incompatibility monotone [34] if it satisfies:

(a) $\mathcal{V}_{\rm I}(\mathcal{M})=0$ if $\mathcal{M}\in$ jointly measurable.

(b) $\mathcal{V}_{\rm I}(\mathcal{M})$ satisfies convexity.

(c) $\mathcal{V}_{\rm I}(\mathcal{M})$ is non-increasing under post-processing, namely

$$\begin{aligned} \{M_{a'|x'}\}_{a',x'} &= \mathcal{W}(\{M_{a|x}\}_{a,x}) \\ &= \sum_{a,x} p(x|x')p(a'|a,x,x')\{M_{a|x}\}_{a,x}. \end{aligned} \tag{19}$$

The condition (a) is automatically satisfied by the difinition of $\mathcal{V}_{\rm I}$:

$$\mathcal{V}_{\rm I}(\{M_{a|x}\}_{a,x}) = \sup_{\rho_B} \mathcal{V}_{\rm S}[\sqrt{\rho_B}\{M_{a|x}\}_{a,x}\sqrt{\rho_B}]. \tag{20}$$

Given that a set of measurements $\{M_{a|x}\}_{a,x}$ is compatible if and only if its SEO induced state assemblage $\sqrt{\rho_B}\{M_{a|x}\}_{a,x}\sqrt{\rho_B}$ can be described by LHS model. Thus, the SIV will vanish.

To prove that (b) $\mathcal{V}_{\rm I}(\mathcal{M})$ satisfies convexity, we only need to demonstrate $\mathcal{V}_{\rm S}(\mathcal{A})$ is convex in assemblage.

Proof. —$C_{\rm d}^{\star}(\mathcal{A})$ satisfies convexity.

Let us consider a convex combination of state assemblages can be described by $\tilde{\mathcal{A}} = q\mathcal{A} + (1-q)\mathcal{A}' := \{q\sigma_{a|x} + (1-q)\sigma'_{a|x}\}_{a,x}$ $\forall q \in [0,1]$. Using the convexity of convexity of $C_{\rm d}$, one can obtain

$$\begin{aligned}
&C_{\rm d}^{\star}(\tilde{\mathcal{A}}) = C_{\rm d}^{\star}\left[q\mathcal{A} + (1-q)\mathcal{A}'\right] \\
&= \max_x \sum_a p(a|x) C_{\rm d}\left[q\rho_{a|x} + (1-q)\rho'_{a|x}\right] \\
&\leq \max_x \sum_a \left[qp(a|x)C_{\rm d}(\rho_{a|x}) + (1-q)p'(a|x)C_{\rm d}(\rho'_{a|x})\right] \\
&\leq q\max_x \sum_a p(a|x)C_{\rm d}(\rho_{a|x}) + (1-q)\max_x \sum_a p'(a|x)C_{\rm d}(\rho'_{a|x}) \\
&= qC_{\rm d}^{\star}(\mathcal{A}) + (1-q)C_{\rm d}^{\star}(\mathcal{A}').
\end{aligned} \tag{21}$$

Following the analogous steps together with the facts that Shannon entropy is concave, we can demonstrate that $H_{\Delta}^{\star}$ is also concave with respect to a convex combination of state assemblages. Therefore, we can conclude that steering violation satisfies convexity, namely

$$\begin{aligned}
&\mathcal{V}_{\rm S}(\tilde{\mathcal{A}}) = \mathcal{V}_{\rm S}\left[q\mathcal{A} + (1-q)\mathcal{A}'\right] \\
&= \max\left\{C_{\rm d}^{\star}[q\mathcal{A} + (1-q)\mathcal{A}'] - H_{\Delta}^{\star}[q\mathcal{A} + (1-q)\mathcal{A}'], 0\right\} \\
&\leq \max\{q\left[C_{\rm d}^{\star}(\mathcal{A}) - H_{\Delta}^{\star}(\mathcal{A})\right] + (1-q)\left[C_{\rm d}^{\star}(\mathcal{A}') - H_{\Delta}^{\star}(\mathcal{A}')\right], 0\} \\
&\leq q\max\left\{\ C_{\rm d}^{\star}(\mathcal{A}) - H_{\Delta}^{\star}(\mathcal{A}), 0\right\} + (1-q)\max\left\{C_{\rm d}^{\star}(\mathcal{A}') - H_{\Delta}^{\star}(\mathcal{A}'), 0\right\} \\
&= q\mathcal{V}_{\rm S}(\mathcal{A}) + (1-q)\mathcal{V}_{\rm S}(\mathcal{A}').
\end{aligned} \tag{22}$$

Here, we use the facts that $C_{\rm d}$ ($H_{\Delta}^{\star}$) is a convex (concave) function and the property of the maximization in order. Therefore, we conclude the proof that $\mathcal{V}_{\rm I}(\mathcal{M})$ satisfies convexity. □

For the third one (c) $\mathcal{V}_{\rm I}(\mathcal{M})$ is non-increasing under post-processing, we consider a post-processing scenario $\mathcal{W}$ defined as a deterministic wiring map [46] as show in Fig. 4:

$$\sigma_{a'|x'} = \mathcal{W}(\sigma_{a|x}) = \sum_{a,x} p(x|x')p(a'|a,x,x')\sigma_{a|x}, \quad \forall a, x, \tag{23}$$

where, $p(x|x')$ and $p(a'|a,x,x')$ are conditional probabilities.

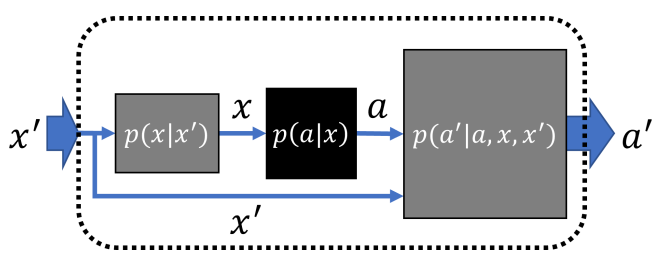

FIG. 4.

To prove $\mathcal{V}_{\rm I}(\mathcal{M})$ is non-increasing under post-processing, we first need to demonstrate that $\mathcal{V}_{\rm S}(\mathcal{A})$ is also non-increasing under post-processing.

Proof. —$\mathcal{V}_{\rm S}(\mathcal{A})$ is non-increasing under post-processing.

We begin this proof by showing that $C_{\mathrm{d}}^{\star}$ is non-increasing under post-processing, that is

$$\begin{aligned}
C_{\mathrm{d}}^{\star}\left[\mathcal{W}(\mathcal{A})\right] &= \max_{x'} \sum_{a'} p(a'|x') C_{\mathrm{d}}\left[\frac{\sigma_{a'|x'}}{p(a'|x')}\right] \\
&= \max_{x'} \sum_{a'} p(a'|x') C_{\mathrm{d}}\left[\sum_{a,x} \frac{p(x|x')p(a'|a,x,x')\sigma_{a|x}}{p(a'|x')}\right] \\
&= \max_{x'} \sum_{a'} p(a'|x') C_{\mathrm{d}}\left[\sum_{a,x} \frac{p(x|x')}{p(a'|x')} \frac{p(a'|x')p(x|x',a')p(a|x,x',a')}{p(x|x')p(a|x,x')} p(a|x)\rho_{a|x}\right] \\
&= \max_{x'} \sum_{a'} p(a'|x') C_{\mathrm{d}}\left[\sum_{a,x} \frac{p(x|x')}{p(a'|x')} \frac{p(a'|x')p(x|x')p(a|x,x')}{p(x|x')p(a|x,x')} p(a|x)\rho_{a|x}\right] \\
&= \max_{x'} \sum_{a'} p(a'|x') C_{\mathrm{d}}\left[\sum_{a,x} \frac{p(a'|x')p(x|x')}{p(a'|x')} p(a|x)\rho_{a|x}\right] \\
&= \max_{x'} \sum_{a'} p(a'|x') C_{\mathrm{d}}\left[\sum_{a,x} p(x)p(a|x)\rho_{a|x}\right] \\
&\leq \max_{x'} \sum_{a'} p(a'|x') \sum_{a,x} p(x)p(a|x) C_{\mathrm{d}}\left(\rho_{a|x}\right) \\
&= \sum_{x} p(x) \sum_{a} p(a|x) C_{\mathrm{d}}\left(\rho_{a|x}\right) \\
&\leq \max_{x} \sum_{a} p(a|x) C_{\mathrm{d}}\left(\rho_{a|x}\right) \\
&= C_{\mathrm{d}}^{\star}(\mathcal{A}).
\end{aligned} \tag{24}$$

Here, we utilize the relation $p(a'|a,x,x') = p(a'|x')p(x|x',a')p(a|x,x',a')/p(x|x')p(a|x,x')$ to arrive at the equation in the third line; in the fourth line, we note that all the labels, say x, x', a should not dependent on a'; in the sixth line, we use the relation of $p(x|x') = p(x)p(x'|x)/p(x') = p(x)$, given that x' should not dependent on x; the seventh line is the convexity of C_{d}.

In contrast, the conditional Shannon entropy increases monotonically after the process due to concavity, namely

$$\begin{aligned}
H_{\Delta}^{\star}\left[\mathcal{W}(\mathcal{A})\right] &= \min_{x'} \sum_{a'} p(a'|x') H_{\Delta}\left[\frac{\sigma_{a'|x'}}{p(a'|x')}\right] \\
&= \min_{x'} \sum_{a'} p(a'|x') H_{\Delta}\left[\sum_{a,x} p(x)p(a|x)\rho_{a|x}\right] \\
&\geq \sum_{a,x} p(x)p(a|x) H_{\Delta}\left(\rho_{a|x}\right) \\
&\geq \min_{x} \sum_{a} p(a|x) H_{\Delta}\left(\rho_{a|x}\right) \\
&= H_{\Delta}^{\star}(\mathcal{A}).
\end{aligned} \tag{25}$$

Combining the results in Eq. (24) and Eq. (25), one can conclude that

$$C_{\mathrm{d}}^{\star}(\mathcal{A}) - C_{\mathrm{d}}^{\star}\left[\mathcal{W}(\mathcal{A})\right] \geq 0 \geq H_{\Delta}^{\star}(\mathcal{A}) - H_{\Delta}^{\star}\left[\mathcal{W}(\mathcal{A})\right], \tag{26}$$

which implies $\mathcal{V}_{\mathrm{S}}(\mathcal{A}) \geq \mathcal{V}_{\mathrm{S}}\left[\mathcal{W}(\mathcal{A})\right]$. □

By using the above result, we can therefore prove that

Proof. —$\mathcal{V}_{\rm I}(\mathcal{M})$ is also non-increasing under post-processing.

$$\begin{aligned}\mathcal{V}_{\rm I}\left[\mathcal{W}(\mathcal{M})\right] &= \sup_{\rho_B} \mathcal{V}_{\rm S}\left[\sqrt{\rho_B}\mathcal{W}(\mathcal{M})\sqrt{\rho_B}\right] \\ &= \mathcal{V}_{\rm S}\left[\sqrt{\rho_B^\star}\mathcal{W}(\mathcal{M})\sqrt{\rho_B^\star}\right] \\ &= \mathcal{V}_{\rm S}\left[\mathcal{W}\left(\sqrt{\rho_B^\star}\mathcal{M}\sqrt{\rho_B^\star}\right)\right] \\ &\leq \mathcal{V}_{\rm S}\left(\sqrt{\rho_B^\star}\mathcal{M}\sqrt{\rho_B^\star}\right) \\ &\leq \sup_{\rho_B} \mathcal{V}_{\rm S}\left(\sqrt{\rho_B}\mathcal{M}\sqrt{\rho_B}\right) \\ &= \mathcal{V}_{\rm I}(\mathcal{M}).\end{aligned} \tag{27}$$

□

Monotonicity of the SIV under GIO

Quantum steering has been articulated within the resource theory framework [46]. A measure $\mathcal{S}$ qualifies as a convex steering monotone if it adheres to the following properties:

(i) $\mathcal{S}(\sigma_{a|x}) = 0$ for all $\sigma_{a|x} \in$ LHS.

(ii) $\mathcal{S}\left[p\sigma_{a|x} + (1-p)\sigma^{'}_{a|x}\right] \leq p\mathcal{S}\sigma_{a|x} + (1-p)\mathcal{S}(\sigma^{'}_{a|x})$ for any real number $0 \leq p \leq 1$ and assemblages $\sigma_{a|x}$ and $\sigma^{'}_{a|x}$.

(iii) Non-increasing under one-way local operations and classical communication:

$$\sum_{\xi} p(\xi)\mathcal{S}\left[\frac{\Xi_\xi(\sigma_{a|x})}{\mathrm{Tr}\Xi(\sigma_{a|x})}\right] \leq \mathcal{S}(\sigma_{a|x}) \quad \forall \sigma_{a|x}, \tag{28}$$

where $p(\xi) = \mathrm{Tr}\Xi(\sigma_{a|x})$ and $\sum_\xi p(\xi) = 1$.

It is clear that $\mathcal{V}_{\rm S}$ satisfies properties (i) and (ii). Nonetheless, for property (iii), we can affirm its adherence only under the limited local operations. The property (iii) states that quantum steering should not increase under the free operations, say, one-way local operations and classical communication [46].

In the scenario of steering-assisted coherence distillation, local operations must also adhere to incoherent operations. In the following, we consider that these local operations belong to the set of genuine incoherent operations [47], which resides as a subset within incoherent operations [16].

As shown in Fig. 5, a local stochastic genuine incoherent operation is performed on Bob's system. Specifically, Bob introduces a device that generates an random outcome ξ with probability $p(\xi)$. After receiving the outcome, Bob sends his system into a corresponding genuinely incoherent operation Ξ_ξ [47], which can be characterized by a set of Kraus operators $\{K_{k,\xi}\}_k$ such that

$$\begin{aligned}&\Xi_\xi(\bullet) = \sum_k K_{k,\xi} \bullet K_{k,\xi}^\dagger \\ \text{with} \quad &\sum_k K_{k,\xi}^\dagger K_{k,\xi} = \mathbb{1}, \\ &K_{k,\xi} = \sum_i c_i^{k,\xi} \left|i\right\rangle \left\langle i\right|.\end{aligned} \tag{29}$$

Additionally, the outcome ξ is also sent to Alice through classical communication, so that she utilizes classical stochastic maps defined by $\{p(a'|a,x,x',\xi), p(x|x',\xi)\}$ to post-process her measurement results. Consequently, the entire process Ξ transforms an initial assemblage $\sigma_{a|x}$ into a final assemblage $\sigma_{a'|x'}$:

$$\begin{aligned}\sigma_{a'|x'} &= \Xi(\sigma_{a|x}) \\ &= \sum_{a,x,\xi} p(x|x',\xi)p(a'|a,x,x',\xi)p(\xi)\Xi_\xi(\sigma_{a|x}).\end{aligned} \tag{30}$$

Note that $\sigma_{a'|x'}$ is a valid state assemblage.

Now, we prove that the SIV is monotonic under this constrain.

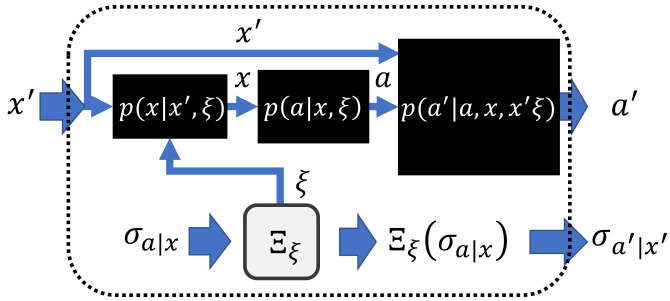

FIG. 5. Schemetic illustration of one-way local genuinely incoherent operations and classical communication.

Proof. —SIV is non-increasing under one-way local genuinely incoherent operations and classical communication.

We aim to use the strategy in Eq. (24) and Eq. (25) by first showing that $C_{\rm d}^\star$ is non-increasing after the process, namely

$$
\begin{aligned}
C_{\rm d}^\star\left[\Xi(\mathcal{A})\right] &= \max_{x'}\sum_{a'} p(a'|x')C_{\rm d}\left[\frac{\sigma_{a'|x'}}{p(a'|x')}\right] \\
&= \max_{x'}\sum_{a'} p(a'|x')C_{\rm d}\left[\sum_{a,x,\xi}\frac{p(x|x',\xi)p(a'|a,x,x',\xi)K_\xi\sigma_{a|x}K_\xi^\dagger}{p(a'|x')}\right] \\
&= \max_{x'}\sum_{a'} p(a'|x')C_{\rm d}\left[\sum_{a,x,\xi}\frac{p(x|x',\xi)}{p(a'|x')}\frac{p(a'|x',\xi)p(x|a',x',\xi)p(a|x,a',x',\xi)}{p(x|x',\xi)p(a|x,x',\xi)}p(a|x)K_\xi\rho_{a|x}K_\xi^\dagger\right] \\
&= \max_{x'}\sum_{a'} p(a'|x')C_{\rm d}\left[\sum_{a,x,\xi}\frac{p(a'|x',\xi)p(x|x',\xi)}{p(a'|x')}p(a|x)K_\xi\rho_{a|x}K_\xi^\dagger\right] \\
&= \max_{x'}\sum_{a'} p(a'|x')C_{\rm d}\left[\sum_{a,x}p(x)p(a|x)\sum_{\xi}p(\xi)\Xi_\xi(\rho_{a|x})\right] \\
&\leq \max_{x'}\sum_{a'} p(a'|x')\sum_{a,x}p(x)p(a|x)C_{\rm d}\left(\sum_{\xi}p(\xi)\Xi_\xi(\rho_{a|x})\right) \\
&\leq \sum_{x}p(x)\sum_{a}p(a|x)C_{\rm d}\left(\sum_{\xi}p(\xi)\rho_{a|x}\right) \\
&\leq \max_{x}\sum_{a}p(a|x)C_{\rm d}\left(\rho_{a|x}\right) \\
&= C_{\rm d}^\star(\mathcal{A}).
\end{aligned}
\tag{31}
$$

Again, in the third line, we utilize the relation: $p(a'|a,x,x',\xi) = p(a'|x',\xi)p(x|a',x',\xi)p(a|x,a',x',\xi)/p(x|x',\xi)p(a|x,x',\xi)$. For the fourth line, label x should not depend on a and label a should not depend on x' and a' as shown in Fig. 5. In the fifth line, we use the relation $p(x) = p(x|x',\xi)p(a'|a,x,x',\xi)/p(a'|x')$ to arrive the equation. In addition, we use the convexity of $C_{\rm d}$ and its monotonic property under incoherent operation [8] to deduce the inequalities in the sixth and the seventh lines, respectively.

In contrast, the $H_\Delta^\star$ will always increase monotonically after the process, namely

$$\begin{aligned}
H_\Delta^\star\left[\Xi(\mathcal{A})\right] &= \min_{x'}\sum_{a'} p(a'|x') H_\Delta\left[\frac{\sigma_{a'|x'}}{p(a'|x')}\right] \\
&= \min_{x'}\sum_{a'} p(a'|x') H_\Delta\left[\sum_{a,x,\xi} p(x)p(a|x)p(\xi)\Xi_\xi(\rho_{a|x})\right] \\
&\geq \sum_{a,x} p(x)p(a|x) H_\Delta\left[\sum_{\xi} p(\xi)\Xi_\xi(\rho_{a|x})\right] \\
&= \sum_{x} p(x)\sum_{a} p(a|x) H_\Delta\left[\sum_{\xi} p(\xi)\left(\sum_{k} K_{k,\xi}\rho_{a|x}K_{k,\xi}^\dagger\right)\right] \\
&= \sum_{x} p(x)\sum_{a} p(a|x) S\left[\sum_{i,k,\xi} p(\xi)|c_i^{k,\xi}|^2 \langle i|\,\rho_{a|x}\,|i\rangle\,|i\rangle\langle i|\right] \\
&= \sum_{x} p(x)\sum_{a} p(a|x) S\left[\Delta(\rho_{a|x})\right] \\
&\geq \min_{x}\sum_{a} p(a|x) H_\Delta\left(\rho_{a|x}\right) \\
&= H_\Delta^\star(\mathcal{A}).
\end{aligned} \tag{32}$$

In this deduction, we use the concavity of the H_Δ and the definition of genuinely incoherent operations in Eq. (29). Therefore, by using the relation similar to Eq. (26), we can conclude that $\mathcal{V}_{\mathrm{S}}(\mathcal{A}) \geq \mathcal{V}_{\mathrm{S}}\left[\Xi(\mathcal{A})\right]$, which ends the proof. □

One can observe that our proof strategy aims to demonstrate $C_{\mathrm{d}}^\star(\mathcal{A}) - C_{\mathrm{d}}^\star\left[\Xi(\mathcal{A})\right] \geq 0 \geq H_\Delta^\star(\mathcal{A}) - H_\Delta^\star\left[\Xi(\mathcal{A})\right]$, which offers a weaker validation of the relationship $C_{\mathrm{d}}^\star(\mathcal{A}) - H_\Delta^\star(\mathcal{A}) \geq C_{\mathrm{d}}^\star\left[\Xi(\mathcal{A})\right] - H_\Delta^\star\left[\Xi(\mathcal{A})\right]$. This is because any Ξ satisfying the former inequality will automatically meet the conditions of the latter inequality. However, the converse is not necessarily true; that is, all Ξ that meet the conditions of the latter inequality may not satisfy the former one. To derive the former inequality, we must limit the local operations to genuinely incoherent operations–a subset of incoherent operations.

Additionally, we have numerically tested the monotonicity of the SIV using 10^7 random pure entangled states ρ^{AB} and random local completely positive and trace-preserving (CPTP) maps Λ on Bob's side. For each pure entangled state, we assume Alice performs Pauli-X: $\hat{\sigma}_1$ and Pauli-Z: $\hat{\sigma}_3$ measurements, i.e., $M_{a|x} = [\mathbb{1}_2 + (-1)^a\hat{\sigma}_x]/2$ with $a \in \{0,1\}$ and $x \in \{1,3\}$. After receiving the assemblage $\mathcal{A} = \{\sigma_{a|x} = p(a|x)\rho_{a|x}\}_{a,x}$, Bob computes both $\mathcal{V}_{\mathrm{S}}(\mathcal{A})$ and $\mathcal{V}_{\mathrm{S}}[\Lambda(\mathcal{A})]$ under the reference basis $\{|i\rangle\}_{i=0,1}$ (eigenbasis of Pauli-Z). Out of all 10^7 random tests, we found 14 cases where the SIV increased after applying the random CPTP map. One of these 14 cases is illustrated below:

$$\rho^{AB} = \begin{pmatrix} 0.276 & 0.293-0.062i & -0.027+0.251i & 0.073-0.203i \\ 0.293+0.062i & 0.325 & -0.085+0.026i & 0.123-0.199i \\ -0.027-0.251i & -0.085-0.026i & 0.230 & -0.191-0.047i \\ 0.073+0.203i & 0.123+0.199i & -0.191+0.047i & 0.168 \end{pmatrix} \tag{33}$$

and CPTP map $\Lambda_1(\rho) = \sum_{i=0}^{3} K_i\rho K_i^\dagger$ with Kraus operators:

$$\begin{aligned}
K_0 &= \begin{pmatrix} 0.559+0.351i & 0.425-0.487i \\ 0.721 & -0.024+0.564i \end{pmatrix}, \quad K_1 = \begin{pmatrix} 0.004+0.021i & 0.388 \\ -0.160-0.030i & 0.319-0.091i \end{pmatrix}, \\
K_2 &= \begin{pmatrix} -0.050-0.071i & 0.032+0.020i \\ 0.097 & 0.005-0.037i \end{pmatrix}, \quad K_3 = \begin{pmatrix} 0.021 & 0.006+0.012i \\ 0.001-0.012i & -0.013-0.016i \end{pmatrix}.
\end{aligned} \tag{34}$$

By calculating the SIVs, we obtain

$$\mathcal{V}_{\mathrm{S}}(\mathcal{A}) \approx 0.061 \quad \text{and} \quad \mathcal{V}_{\mathrm{S}}[\Lambda_1(\mathcal{A})] \approx 0.198, \tag{35}$$

whcih demonstrates that the SIV increases after the CPTP map. However, when applying this map to a maximally mixed state $\mathbb{1}/2$, we find that

$$\Lambda_1\left(\frac{\mathbb{1}}{2}\right) = \begin{pmatrix} 0.506 & 0.117+0.026i \\ 0.117-0.026i & 0.494 \end{pmatrix}, \tag{36}$$

which implies that $\Lambda_1 \notin \text{ICO}$. In fact, $\Lambda_1[\rho_{\text{I}}(\alpha)] \notin \text{ICO}\ \forall \rho_{\text{I}} = \alpha\,|0\rangle\langle 0| + (1-\alpha)\,|1\rangle\langle 1| \ \in \mathcal{I}\ \forall \alpha \in [0,1]$

After reviewing all other cases with a similar method, we conclude from the numerical tests that the SIV could be non-increasing under one-way local incoherent operations and classical communication [16].

SIV examples: Werner state and Rank-2 Bell diagonal state

Here, we provide examples of the violation or witness with two-qubit Werner and Bell diagonal states. The two-qubit Werner state is characterized by mixtures of a maximally entangled state and a maximally mixed state, namely

$$\rho^{\text{Werner}}(w) = w\,|\beta^{11}\rangle\langle\beta^{11}| + (1-w)\frac{\mathbb{1}}{2}\otimes\frac{\mathbb{1}}{2}, \tag{37}$$

where $|\beta^{uv}\rangle = [|0\rangle\otimes|v\rangle + (-1)^u\,|1\rangle\otimes|1\oplus v\rangle]/\sqrt{2}$ for $u,v\in\{0,1\}$ are Bell states and $w\in[0,1]$. Note, we use the notation $|u\oplus v\rangle = |u+v \mod 2\rangle$.

We consider that Alice performs Pauli-X and Pauli-Z measurements, where the measurement operators are $M_{a|x} = [\mathbb{1}_2 + (-1)^a\hat{\sigma}_x]/2$ with $a\in\{0,1\}$ and $x\in\{1,3\}$. Here $\hat{\sigma}_1$, $\hat{\sigma}_2$, and $\hat{\sigma}_3$ are Pauli-X, Pauli-Y, and Pauli-Z matrices, respectively. The output state assemblage after the measurement can be written as

$$\sigma^{\text{Werner}}_{a|x}(w) \quad = \frac{1}{2}\left[\frac{1}{2}\mathbb{1} + \frac{w}{2}(-1)^a\hat{\sigma}_2\hat{\sigma}_x\hat{\sigma}_2\right], \tag{38}$$

with the probabilities $\text{Tr}[\sigma^{\text{Werner}}_{a|x}(w)] = 1/2\ \forall a,x$. According to Eq. (6), the steering violation of Werner state reads

$$\mathcal{V}_{\text{S}}[\mathcal{A}^{\text{Werner}}(w)] = \max\left\{1 + 2(1-\frac{w}{2})\log_2(1-\frac{w}{2}) + w\log_2\frac{w}{2}, 0\right\}. \tag{39}$$

The violation successfully detects quantum steering when $w > 0.779$, which is shown in Fig. 6. Note that as reported in Ref. [41], there exist steering witnesses, for which the steerability can be detected when $w > 1/\sqrt{2} \approx 0.707$ under two measurement settings.

Let us now consider the rank-2 Bell-diagonal state, i.e., a mixture of different types of Bell states, namely

$$\rho^{\text{Bell}}(w) = w\,|\beta^{11}\rangle\langle\beta^{11}| + (1-w)\,|\beta^{01}\rangle\langle\beta^{01}|, \tag{40}$$

which is steerable for $w\in(0.5,1]$ [33]. The state assemblage received by Bob can be written as

$$\sigma^{\text{Bell}}_{a|x}(w) = \frac{w}{2}\hat{\sigma}_2 M^T_{a|x}\hat{\sigma}_2 + \frac{1-w}{2}\hat{\sigma}_3\hat{\sigma}_2 M^T_{a|x}\hat{\sigma}_2\hat{\sigma}_3 \tag{41}$$

with the probabilities $\text{Tr}\sigma^{\text{Bell}}_{a|x}(w) = 1/2$ for all a,x. The corresponding steering violation can be expressed by

$$\mathcal{V}_{\text{S}}[\mathcal{A}^{\text{Bell}}(w)] = 1 + (1-w)\log_2(1-w) + w\log_2 w \tag{42}$$

We plot the violation values for $w\in[0.5,1]$ as the blue-dash-dot curve in Fig. 6. In Fig. 6, we observe that there is a sudden-death effect of the steering violation of Werner state at $w\approx 0.779$. This suggests that the violation cannot detect all steerable Werner state as reported in Ref. [41]. In contrast, the violation successfully witnesses all steerable rank-2 Bell-diagonal state for $w\in(0.5,1]$ [60].

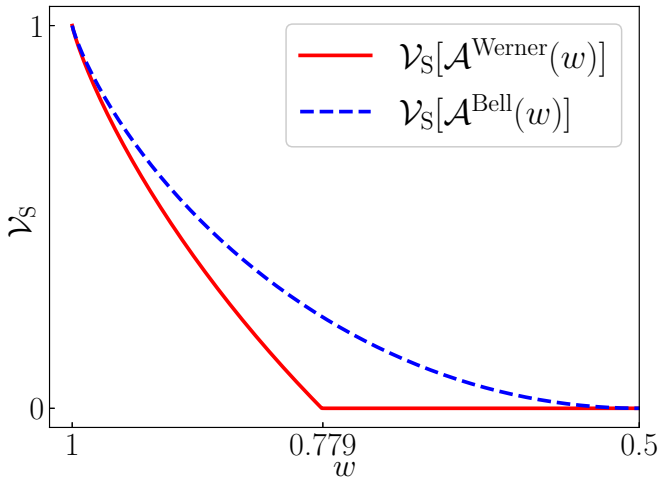

FIG. 6. The violation of the two different bipartite states. The blue-dash curve represents the violation value of the rank-2 Bell-diagonal state, showing all steerable rank-2 Bell-diagonal states for $w > 0.5$; the red-solid curve represents the violation value of the Werner state, which has a sudden-death effect at $w \approx 0.779$ and indicates steerability for $w > 0.779$.